

Polyelectrolyte-Catalyzed Acetyl Transfer Reactions. Aminolysis of Phenyl Acetates by Poly(ethylenimine): Catalytic, Inhibition, and Solvent Effects and Thermodynamic Parameters

Antonio Arcelli

Dipartimento di Chimica "G. Ciamician", via Selmi, 2-40126 Bologna, Italy

ABSTRACT: The kinetics of the aminolysis of selected phenyl acetates in an excess of poly(ethylenimine) (PEI) were studied at 25 °C in aqueous solution at various pH values. The neutral esters 2-nitrophenyl acetate (NPA) and 2,4-dinitrophenyl acetate (DNPA), showed saturation kinetics vs PEI concentration. The substrate–polyelectrolyte binding constant (K_1) as well as the decomposition rate constant (k_{cat}) of the complex (X_1) which yields acetylated PEI and phenol were determined. The aminolysis of 4-acetoxy-3-nitrobenzenesulfonate (ANBS) and 3-acetoxy-2,6-dinitrobenzoic acid (ADNB) showed a more complicated rate behavior: the rate increased as the PEI concentration increased, passed through a maximum, and then decreased. These results were explained by the formation of the ordinary complex (X_1) and by an additional unreactive complex (X_2). An equation was elaborated that allowed the evaluation of (a) the binding constant (K_1), (b) the decomposition rate (k_{cat}) of X_1 , and (c) the unreactive complex inhibition constant (K_2). Unlike the case of neutral esters, the Brønsted-type plots obtained for the ANBS and ADNB complex decomposition (X_1) were not linear. The most likely mechanism involves the formation of a zwitterionic tetrahedral intermediate T^\pm (Scheme 3) along the reaction path. A semiempirical equation based on this hypothesis fits the experimental data well. A detailed examination of a possible more general reaction scheme, the estimation of pK values of intermediates and structure–reactivity considerations, showed that intramolecular general base and/or general acid catalysis are unimportant. Solvent effect and activation parameters were discussed.

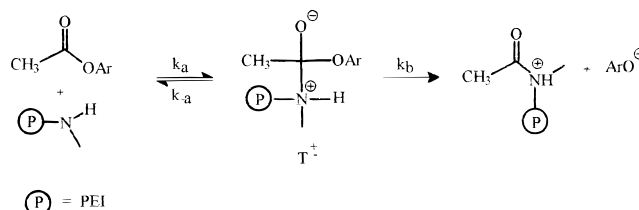
Introduction

In the past, several authors examined the influence of synthetic polyelectrolytes on the decomposition rate of activated esters¹ with the aim of providing a better understanding of complex enzymatic processes.² However, despite the considerable effort made in this direction, an exhaustive description of the reaction mechanisms of polyelectrolyte-catalyzed acetyl transfer is still lacking. For instance, it is not clear whether the aminolysis occurs stepwise or proceeds through a concerted path; moreover, the relative contribution of general acid base catalysis has never been well established.

Much work has been carried out with polyelectrolytes containing amino, imidazole, and pyridine groups.³ Klotz et al.⁴ studied the influence of poly(ethyleneimine) grafted with imidazole and 2-(dimethylamino)ethyl in the hydrolysis of 4-nitrophenyl caproate and hypothesized the presence of cooperative effects. Also, Overberger et al.⁵ reported that the hydrolysis of *p*-nitrophenyl acetate catalyzed by poly[4(5)-vinylimidazole] probably involves a general base catalysis of attack of the pendant imidazole groups on the ester.

Recently,^{6,7} we have found that the kinetic of aminolysis of selected phenyl acetates by poly(ethylenimine) (PEI) in 1 M KCl follows, at a given pH, the linear equation $k_{\text{obs}} = k_0 + k_2 [\text{PEI}_{\text{tot}}]$, where k_2 is the second-order rate constant for the uncatalyzed nucleophilic reaction and k_0 is the rate constant for the spontaneous hydrolysis. By changing the pH, the polyelectrolyte behaves as a simple monomeric amine of different basicity, and so it was possible to use Brønsted-type correlations as mechanistic criteria to hypothesize a reaction mechanism involving the formation of a tetrahedral intermediate T^\pm accompanied by a change in the

Scheme 1



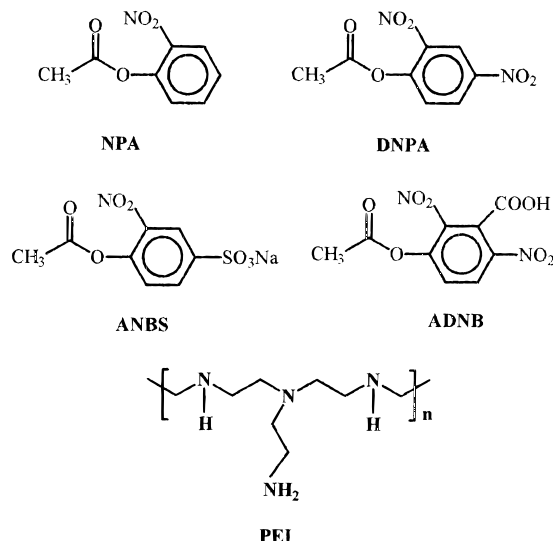
rate-determining step⁷ along the reaction pathway (Scheme 1).

Unfortunately, in the absence of electrolyte the matter is much more complicated because the large electrostatic field surrounding the macroion affects the distribution and the reactivity of the reactants (especially those of opposite charge to the polyelectrolyte), and specific interactions may operate.⁸ These effects may lead to large accelerations or decelerations, and the kinetic behavior is not easy to evaluate.

In this paper we analyze the behavior of the PEI in the aminolysis reactions of some neutral and anionic phenyl acetates at various pH values in the absence of simple strong electrolytes. Our aim is directed at better understanding the details of reaction mechanisms in a system in which the substrate–polyelectrolyte interactions (i.e., dipolar or electrostatic, hydrogen bonding, etc.) affect, in some cases also dramatically, the reaction rate. To avoid altering the electrostatic field around the macroion by the addition of the salt,⁶ we did not maintain the ionic strength I constant. This procedure seemed inevitable, taking into account that the presence of the strong electrolyte (KCl), even at low concentrations, suppressed the substrate–polyelectrolyte interactions.⁶ Besides, the change in the ionic strength I has a negligible effect on the aminolysis of phenyl acetates

with simple monomeric amines,⁹ and the contribution of highly charged polyions and its counterions to the ionic strength I cannot be estimated unambiguously.^{10a}

On the basis of Brønsted correlations, the evaluation of microscopic rate constants of the various reaction pathways, the determination of thermodynamic parameters, and the investigation of solvent effects, it is possible to gain further insight into the mechanism of acetyl transfer in a complicated system such as PEI in which the reagent represents a whole family of nucleophiles and general base/acid catalysts.



Experimental Section

Materials. 2-Nitrophenyl acetate, 2,4-dinitrophenyl acetate, 4-acetoxy-3-nitrobenzenesulfonate (sodium salt), 3-acetoxy-2,6-dinitrobenzoic acid, 4-acetoxy-3-chlorobenzoic acid, and 4-acetoxybenzoic acid were prepared or purchased as previously reported.⁷ Other products (Aldrich or Merck) were of analytical grade. Poly(ethylenimine) (PEI) was "Polymin P" from B.D.H. with a monomer molecular weight of 59 determined as previously reported.⁷ Deionized water was redistilled from KMnO₄. PEI buffer solutions were prepared in the absence and/or the presence of 1 M KCl (pH = 8.40) in water or in 42.8 (w/w) % CH₃CN/H₂O under nitrogen atmosphere. The pH value (± 0.02) was adjusted by the addition of 0.05–5 M HCl in a thermostated bath and was checked after half an hour. The solutions were used within 1 day.

Potentiometric Titrations. All potentiometric titrations were performed with 0.05–9.29 M HCl in a thermostated bath at 25 ± 0.2 °C under nitrogen atmosphere. A syringe microburet type SB2 titration equipment and a Knick pH-meter model 643 fitted with an Ingold HA-405 combined glass electrode (standardized as reported in ref 11) were used. In the mixed solvent, the glass electrode was standardized at 25 °C with a 0.05 M potassium hydrogen phthalate buffer in 42.8 (w/w) % CH₃CN/H₂O at pH* = 5.22 (calculated from data in ref 12).

PEI is a branched polymeric amine with a very compact structure and only a limited possibility of expansion. It contains 25% primary, 50% secondary, and 25% tertiary amino groups.^{10b–d} Due to electrostatic interactions and the different nature of ionizable groups present in the chain, the apparent dissociation constant pK_n depends on the polyion concentration, the ionization degree, and the ionic strength of the solution.^{10b,c} At each observed pH value the apparent pK_n of the conjugate acid of the PEI amino groups was determined by the equation $pK_n = \text{pH} + \log \alpha/(1 - \alpha)$ where α is the ionization degree calculated as reported in refs 7 and 10c. The mean values of six to nine pK_n values, calculated at various PEI concentrations and pH values, are reported in Table 1.

Kinetic Methods. Kinetic studies were carried out at 25 ± 0.1 °C at various pH values. PEI was used in excess in order

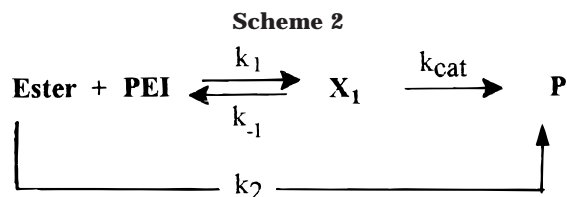
to determine the pseudo-first-order rate constant. The phenol or phenolate released was monitored spectrophotometrically on a Lambda 6 Perkin-Elmer spectrophotometer. Fast kinetics ($t_{1/2} < 30$ s) were measured with a dual-wavelength spectrophotometer Sigma-ZW II (Biochem) equipped with a thermostated stopped-flow unit.⁷ The final ester concentrations were in the range 10^{-4} – 10^{-5} M. For slower reactions, optical density end points were obtained after 10 half-lives, keeping the reaction at 50 °C. On taking the measurements, a decrease of less than 0.1 pH units was observed. The pseudo-first-order rate constants (k_{obs}) were obtained according to the Guggenheim¹³ method or were calculated by a least-squares routine from the slope of the plot $\log (OD_{\infty} - OD_0)/(OD_{\infty} - OD_t)$ vs time. The reaction products, acetylated PEI and phenol, were determined as described in a previous paper.⁷

Other experimental details and data are reported in Table 1 and in Figures 1 and 3. The kinetic constants are average values of two or three experiment distributed in a range of 3%.

Thermodynamic and Activation Parameters. The thermodynamic and activation parameters for the catalyzed ($k_{\text{cat}}K_1$) and uncatalyzed (k_2) process were determined from kinetic data obtained in the aminolysis of the NPA and the ANBS in PEI at pH = 8.40 at four or five different temperatures between 15.5 and 40.1 °C. The free energy of activation was calculated by using the expression $\Delta F^\ddagger = RT \ln(kT/hk)$. Enthalpy, unitary free energy, and unitary entropy changes were obtained from the relationships $\ln K_1 = -\Delta H/RT + C$, $\Delta F_u = -RT \ln K_1 - 7.98 T$, and $\Delta S_u = \Delta S + 7.98$.^{14,15} The values are summarized in Table 2.

Results and Discussion

Aminolysis of 2-Nitrophenyl Acetate (NPA) and 2,4-Dinitrophenyl Acetate (DNPA). The pseudo-first-order rate constants (k_{obs}) were determined in the pH range 4.55–10.70 at various PEI concentrations between 0.015 and 0.882 monomer mol L⁻¹. As found in the hydrolysis of other phenyl acylates with unmodified and modified polyethylenimine^{4,16a,b} and/or poly(1-methyl-5-vinyl imidazole),^{17a} saturation kinetics were observed for both esters. Examples are illustrated in Figure 1. The results are consistent with an association of the substrate with the polymer in a preequilibrium step to give a complex (X_1) that undergoes a reaction to afford acetylated PEI and phenol as in the uncatalyzed process (Scheme 2).^{6,18}



$K_1 = k_1/k_{-1}$ is the binding constant for the substrate–polyelectrolyte association, and k_{cat} is the first-order rate constant for the X_1 decomposition to products. By using an excess of PEI and assuming that $k_{\text{cat}} \ll k_{-1}$, an expression for the reaction rate of Scheme 2 is given by eq 1.^{6,18}

$$k_{\text{obs}} = \frac{k_{\text{cat}}K_1[\text{PEI}]}{1 + K_1[\text{PEI}]} \quad (1)$$

The values of K_1 and k_{cat} were determined by a nonlinear curve fitting of k_{obs} vs [PEI] using the FigP program (Biosoft).

The results are reported in Table 1. Increasing the pH value for both esters, we observed a decrease in the

Table 1. Experimental Conditions and Kinetic Parameters for the Aminolysis Reaction of Selected Phenyl Acetates in an Aqueous Solution of Poly(ethylenimine) (PEI) at 25 °C

pH	λ^a/nm	[PEI]/[monomer]/ mol L^{-1}	pK_n^b	$(1 - \alpha)^c$	no. of runs	K_1/M^{-1}	$k_{\text{cat}}/\text{s}^{-1}$	K_2/M^{-1}
2-Nitrophenyl Acetate^d								
4.55	350	0.015–0.796	5.19	0.19	6	71 ± 14	$(7.8 \pm 0.5) \times 10^{-5}$	
5.75	350	0.015–0.80	6.12	0.30	14	31 ± 6	$(8.9 \pm 0.2) \times 10^{-4}$	
6.88	420–550	0.02–0.804	7.01	0.43	7	39 ± 5	$(6.9 \pm 0.2) \times 10^{-3}$	
6.88 ^e	420–550	0.00565–0.713	7.05 ^f				$(1.85 \pm 0.2) \times 10^{-4g}$	
7.82	420–440	0.031–0.313	7.60	0.63	12	14 ± 1	$(5.3 \pm 0.1) \times 10^{-2}$	
8.40	420–550		8.00			4.0 ± 0.6^h	0.22 ± 0.02^h	
9.10	420–550	0.027–0.27	8.30	0.86	12	1.7 ± 0.3	0.82 ± 0.3	
10.70	420–550	0.057–0.882	8.76		12		1.66 ± 0.03^g	
8.40								
at 15.5 °C	420–550	0.060–0.90			8	5.1 ± 0.7	0.10 ± 0.01	
at 19.9 °C	420–550	0.057–0.802			8	4.3 ± 0.4	0.15 ± 0.01	
at 30 °C	420–550	0.056–0.803			9	3.4 ± 0.4	0.38 ± 0.03	
8.40								
in 1 M KCl	420–550	0.0616–0.535			6		$(6.6 \pm 0.3) \times 10^{-2g}$	
at 20.3 °C								
at 25 °C							9.9×10^{-2h}	
at 30.1 °C	420–550	0.0618–0.537			8		0.19 ± 0.03^g	
at 40.1 °C	420–550	0.062–0.538			9		0.45 ± 0.02^g	
2,4-Dinitrophenyl Acetate^d								
5.02	422	0.0297–0.270	5.49	0.25	12	22 ± 3	$(6.4 \pm 0.3) \times 10^{-3}$	
6.67	422–550	0.0277–0.271	6.81	0.42	10	21 ± 2	$(8.9 \pm 0.2) \times 10^{-2}$	
7.30	422–550	0.0293–0.270	7.28	0.51	12	19 ± 4	0.26 ± 0.02	
7.85	422–550	0.0279–0.2817	7.61	0.63	18	15 ± 1	0.68 ± 0.02	
8.40	422–550		8.07	0.69		5.0 ± 0.6^h	2.2 ± 0.1^h	
9.10	422–550	0.027–0.27	8.31	0.86	12	3.3 ± 1	6.2 ± 1.2	
9.90	422–550	0.035–0.32	8.63	0.95	14	15 ± 2	2.1 ± 0.1	
10.70	422–550	0.057–0.882	8.76	0.99	14	1.3 ± 0.3	18 ± 2.0	
4-Acetoxy-3-nitrobenzenesulfonateⁱ								
3.00	377	0.004–0.0502	4.18	0.07	6	25 ± 11	$(2.8 \pm 0.2) \times 10^{-3l}$	
4.00	400–650	0.000342–0.089	4.95	0.12	13	$(3.8 \pm 1.0) \times 10^3$	$(7.2 \pm 0.7) \times 10^{-2}$	150 ± 39
5.00	400–650	0.000936–0.072	5.46	0.26	15	$(1.9 \pm 0.7) \times 10^3$	0.43 ± 0.05	190 ± 38
6.20	400–65	0.000936–0.056	6.32	0.43	15	$(1.8 \pm 0.3) \times 10^3$	1.40 ± 0.05	50 ± 5
6.67	400–650	0.00217–0.072	6.70	0.50	12	$(4.9 \pm 0.8) \times 10^2$	4.2 ± 0.2	68 ± 7
7.20	400–650	0.00549–0.0738	7.05	0.59	13	$(1.6 \pm 0.4) \times 10^2$	8.3 ± 1.1	68 ± 12
7.20 ^e	420–600	0.0029–0.0645	7.15 ^f		11	$(1.0 \pm 0.1) \times 10^3$	21 ± 1	
7.80	400–650	0.0369–0.072	7.40	0.71	11	$(1.5 \pm 0.2) \times 10^2$	9.6 ± 0.8	22 ± 4
8.40	400–650		7.77	0.81		92 ± 14	9.1 ± 0.8	4.5 ± 2
9.13	400–650	0.0072–0.0432	8.11	0.91	7	30 ± 4	11 ± 0.8	
10.02	400–650	0.045–0.0954	8.48	0.97	8	66 ± 4	2.0 ± 0.1	
10.70	400–650	0.0567–0.882	8.76	0.99	12	4.0 ± 0.6	12 ± 0.8	
8.40								
at 30 °C	400–650	0.00207–0.072			20	90 ± 9	9.3 ± 0.4	
at 35.1 °C	400–650	0.0036–0.145			24	$(1.0 \pm 0.1) \times 10^2$	9.5 ± 0.7	
at 40 °C	400–650	0.00207–0.076			20	95 ± 9	12 ± 0.5	
8.40 in 1 M KCl								
at 20 °C	400–650	0.0396–0.36			15		0.79 ± 0.2	
at 30.1 °C	400–650	0.0378–0.36			15		2.1 ± 0.1^g	
at 35 °C	400–650	0.0459–0.607			16		3.3 ± 0.1^g	
at 40.1 °C	400–650	0.0396–0.18			12		3.9 ± 0.2^g	
3-Acetoxy-2,6-dinitrobenzoic Acidⁱ								
3.00	377	0.004–0.0502	4.18	0.07	9	90 ± 15	$(2.2 \pm 0.1) \times 10^{-2m}$	
4.01	377–550	0.00048–0.0072	4.95	0.12	18	$(3.1 \pm 0.4) \times 10^3$	0.52 ± 0.02	155 ± 15
5.02	377–550	0.00054–0.036	5.43	0.27	20	$(6.4 \pm 1.0) \times 10^3$	1.3 ± 0.05	55 ± 4
5.20	377–550	0.0004–0.0054	5.71	0.29	18	$(2.3 \pm 0.4) \times 10^3$	2.1 ± 0.1	195 ± 30
5.84	377–550	0.00054–0.0045	6.05	0.38	18	$(2.2 \pm 0.3) \times 10^3$	6.4 ± 0.4	190 ± 30
6.25	377–550	0.0043–0.0747	6.34	0.44	22	$(8.2 \pm 0.4) \times 10^2$	8.61	47 ± 9
6.67	377–550	0.00189–0.054	6.70	0.50	18	$(2.8 \pm 0.2) \times 10^3$	7.4 ± 0.1	15 ± 0.5
7.45	377–550	0.00423–0.0396	7.17	0.65	22	$(9.2 \pm 0.1) \times 10^2$	17 ± 0.2	11 ± 1
8.40	377–550		7.77			70 ± 7^h	30.5 ± 1.7^h	
10.02	377–550	0.00413–0.072	8.48	0.972	20	$(3.7 \pm 0.3) \times 10^2$	1.8 ± 0.2	
10.70	377–550	0.060–0.882	8.76	0.99	12	7.5 ± 0.5	18 ± 1	
4-Acetoxy-3-nitrobenzoic Acidⁱ								
6.67	410–550	0.0027–0.036	6.81	0.4	20	$(1.1 \pm 0.4) \times 10^2$	3.3 ± 0.8	140 ± 46
4-Acetoxy-3-chlorobenzoic Acidⁱ								
6.67	280–350	0.027–0.36	6.81	0.4	20	$(8.5 \pm 0.3) \times 10^2$	0.25 ± 0.02	67 ± 12
4-Acetoxybenzoic Acidⁱ								
6.67	280	0.0026–0.042	6.81	0.4	20	$(4.7 \pm 0.1) \times 10^2$	$(1.9 \pm 0.2) \times 10^{-2}$	78 ± 12

^a Analytical wavelength; reactions were followed by single- or dual-wavelength spectroscopy. ^b The values (0.05) were calculated by equation $pK_n = \text{pH} - \log(1 - \alpha)/\alpha$. ^c Free base fraction of macroion mean value. ^d Kinetic parameters were calculated from eq 1 (see text); standard errors are reported. ^e Kinetics followed in a 42.8 (w/w) % CH₃CN/H₂O mixed solvent. ^f pK_n calculated in mixed solvent at [PEI] = 0.05 monomer mol⁻¹ L⁻¹ from titration curve. ^g Value of the second-order rate constant (k_2) calculated from equation $k_{\text{obs}} = k_0 + k_2[\text{PEI}]_{\text{tot}}$. ^h From ref 6. ⁱ Kinetic parameters were calculated from eq 3. ^j The values of k_{obs} at various [PEI] concentrated were corrected for the spontaneous hydrolysis ($k_0 = 1.86 \times 10^{-4} \text{ s}^{-1}$, determined in 0.05 M HCOOH/HCOONa buffer at ionic strength $I = 0.5$ with KCl). ^m The spontaneous hydrolysis ($k_0 = 1.80 \times 10^{-4} \text{ s}^{-1}$) was negligible.

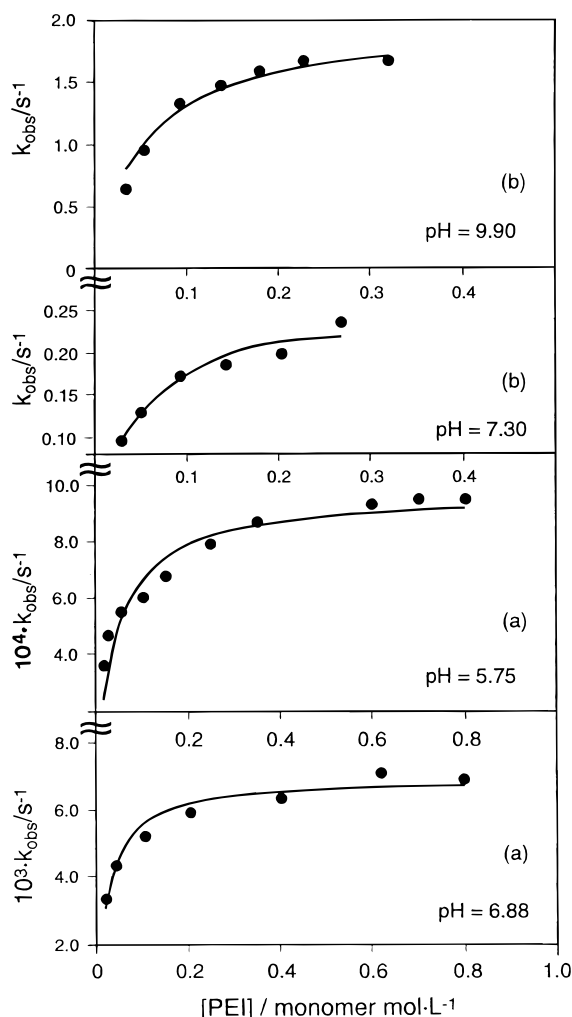


Figure 1. Dependence of the pseudo-first-order rate constant (k_{obs}) on the PEI concentration for the aminolysis of NPA (a) and DNPA (b) at various pH at 25 °C. The points are experimental, and the lines represent the best fit obtained by means of eq 1 using the parameters given in Table 1.

Table 2. Thermodynamic and Activation Parameters for the Aminolysis Reaction of 2-Nitrophenyl Acetate (NPA) and 4-Acetoxybenzenesulfonate (ANBS) by Poly(ethylenimine) at pH = 8.40^a

parameter	$\Delta F^\ddagger /$ kJ mol ⁻¹ ^b	$\Delta H^\ddagger /$ kJ mol ⁻¹ ^c	$\Delta S^\ddagger /$ J K ⁻¹ mol ⁻¹ ^d	$T\Delta S^\ddagger /$ kJ mol ⁻¹
2-Nitrophenyl Acetate				
$K_1 k_{\text{cat}}$	73 ± 6	44 ± 4	-98 ± 13	-29.2 ± 4.6
k_{cat}	77 ± 6	63 ± 4	-45 ± 12	-13.3 ± 4.1
K_1^e	-13.4 ± 4.1 ^f	-19.2 ± 2.1	-19.7 ± 8.3 ^g	
k_2^h	79 ± 5	72 ± 3	-20 ± 10	-5.8 ± 2.9
4-Acetoxy-3-nitrobenzenesulfonate				
$K_1 k_{\text{cat}}$	56 ± 1	10.5 ± 0.8	-154 ± 3	-4.6 ± 1
k_{cat}	68 ± 5	20.5 ± 4.2	-159 ± 12	-48 ± 4
K_1^e	-21.8 ± 4.1 ^f	-9.6 ± 4.6	41 ± 8 ^g	
k_2^h	72 ± 9	64 ± 7	-29.3 ± 6.2	-8.8 ± 2.5

^a Calculated from data in Table 1. Standard errors are reported.

^b $\Delta F^\ddagger = RT \ln(kT/hk)$. ^c $\Delta H^\ddagger = E_a - RT$. ^d $\Delta S^\ddagger = (\Delta H^\ddagger - \Delta F^\ddagger)/T$. ^e $\log K_1 = -\Delta H/RT + \Delta S/R$. ^f Values of unitary free energy and entropy change.^{14,15} ^g Values of unitary free energy and entropy change.^{14,15} ^h Second-order rate constant for the uncatalyzed process calculated from $k_{\text{obs}} = k_0 + k_2[\text{PEI}_{\text{tot}}]$ measured in 1 M KCl.

substrate binding K_1 which is associated with an increase in the complex X_1 decomposition rate k_{cat} . For NPA at pH = 10.70, K_1 is no longer detectable as shown by the linear dependence of k_{obs} vs PEI concentration,

and for the DNPA at pH > 9.10 a nonmonotonic behavior of K_1 was observed. The values of K_1 are relatively low, suggesting that weak substrate–polyelectrolyte interactions are present.

This interpretation is in agreement with the negative ΔH^\ddagger (-19.2 kJ mol⁻¹) and ΔS^\ddagger (-19.7 J K⁻¹ mol⁻¹) values of substrate–polyelectrolyte binding (K_1) determined for NPA at pH = 8.40 (Table 2). In fact, as reported in the literature,^{14,19} hydrophobic interactions would require positive values of ΔS^\ddagger . In the catalytic process the rate of complex decomposition X_1 (k_{cat}) has a smaller activation enthalpy and entropy ($\Delta H^\ddagger = 63$ kJ mol⁻¹, $\Delta S^\ddagger = -45$ J K⁻¹ deg⁻¹) than in the uncatalyzed process (k_2) ($\Delta H^\ddagger = 72$ kJ mol⁻¹, $\Delta S^\ddagger = -20$ J K⁻¹ deg⁻¹). The lower value of ΔS^\ddagger might indicate a reorganization of the polyelectrolyte. The proximity of ΔF^\ddagger values for the two processes suggests that similar mechanisms are involved.

The considerable catalysis of PEI in the absence of the strong electrolyte (KCl) is demonstrated by the comparison of $k_{\text{cat}}K_1$ with the second-order rate constant for the uncatalyzed process k_2 . For example, in the case of NPA, the $(k_{\text{cat}}K_1)/k_2$ ratio is 43 at pH = 8.40 and 3.4×10^2 at pH = 4.55.²⁰

A quantitative evaluation of these rate enhancements is not possible at present. However, we can deduce the reaction mechanism on the basis of the Brønsted-type relationship and through the estimation of the rate constants for the possible reaction pathways.

The Brønsted-type relationship which correlates the rate constants with the basicity of the nucleophile is a measure of the sensitivity of the reaction to the strength of the base and can demonstrate the existence of a change in the rate-determining step.^{21a,22c} It can be obtained by using the rate constant k_{cat} which reflects the reactivity of the complex. It is possible to compare k_{cat} with the bimolecular uncatalyzed process k_2 by means of the ratio $k_{\text{cat}}/[\text{PEI}]_i$ in which $[\text{PEI}]_i$ is the intramolecular concentration of free amino groups catalyzing the reaction in the complex. $[\text{PEI}]_i$ is independent of the total polyamine concentration but depends on the availability and basicity of the amino groups in the complex, which are both functions of the degree of ionization α of the polyelectrolyte. Thus, the dependence of the complex reactivity on the pK_n value of the amino groups can be expressed by the equation $k'_{\text{cat}} = k_{\text{cat}}/(1 - \alpha)$ where α is the mean degree of ionization at each pH value in the range of the PEI concentrations used and $(1 - \alpha)$ is the fraction of free amino groups that catalyze the reaction. The statistically uncorrected Brønsted-type plots,⁷ obtained by plotting the logarithms of k'_{cat} as a function of pK_n 's of the PEI and shown in Figure 2, are linear with slope $\beta_n = 1.05$ for the NPA and 0.85 for the DNPA. These values are close to those obtained for the uncatalyzed reaction with PEI⁷ and for the aminolysis of phenyl acetates with simple amines ($\beta_n = 0.9 \pm 0.1$).^{22a-d} This means that the sensitivity of the reaction rate to the PEI basicity is similar to that of the bimolecular process, and it is independent of the nature of the catalyzing amino groups in the chain (primary, secondary, or tertiary). Moreover, the increase in the reactivity of the complex k'_{cat} , which, for example, is more than 2×10^3 times higher for the NPA when the pH changes from 4.55 to 9.10, depends more on the PEI basicity ($pK_n = 5.19$ and 8.30) than on its effective molarity (EM),^{21b,23} which at the two pH's is 19 or 4.88 M, respectively (see Ap-

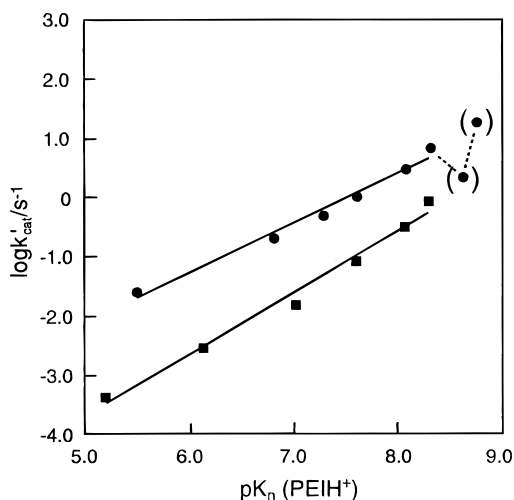


Figure 2. Brønsted-type plots of $\log k_{\text{cat}}$ vs pK_n for the aminolysis of NPA (■) and DNPA (●) by PEI at 25 °C. In parentheses points not computed (see text).

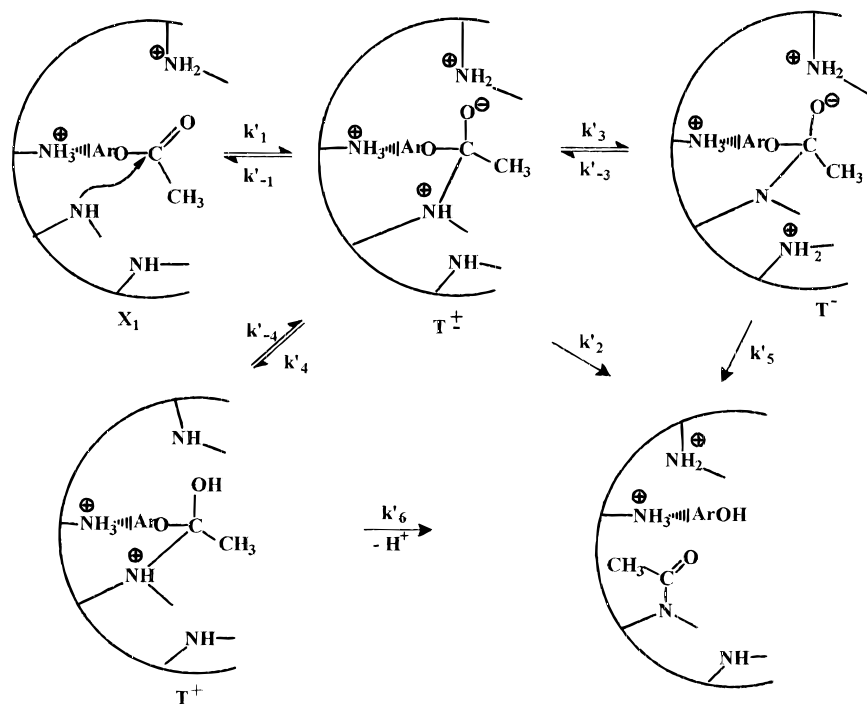
pendix). In the case of DNPA, the linear deviations of k_{cat} observed on the plot, at $pK_n = 8.63$ and 8.76 , reflect the nonmonotonic behavior of the values of the binding constant K_1 at $pH > 8.40$ (see Table 1). This fact and the relatively low basicity of the PEI in the absence of a strong electrolyte^{10b,c} does not allow the kinetic analysis to be extended to higher pH values in order to verify the curvature in the Brønsted-type plot and to establish a concerted nature of the reaction. However, the large dependence of the rate constants on PEI basicity indicates that the aminolysis reaction of the complex X_1 proceeds stepwise with the formation of a zwitterionic tetrahedral intermediate T^\pm by a nucleophilic attack of the amino group of the macroion on the ester. The rate-determining step results in the breakdown of the addition intermediate T^\pm to the products (k_2), which requires a large amount of bond formation

and a charge development on the attacking amine (see Scheme 3).^{22a-c}

This interpretation does not exclude that a possible alternative process involving intramolecular base and/or acid catalysis may occur as shown in Scheme 3. In fact, the T^\pm intermediate can undergo intramolecular proton transfer to give T^- (through the microscopic constant k_3) and/or T^+ (through the microscopic constant k_4) and go to the reaction products. The importance of the two processes can be evaluated from the comparison of the estimated values of k_3 and k_4 with the rate constant k_2 for the decomposition of the T^\pm to the reaction products (see Appendix). In the case of the NPA, only at $pH = 9.10$, the value of $k_3[\text{PEI}]_i = 3.3 \times 10^{10} \text{ s}^{-1}$ for the intramolecular base catalysis was higher than the value of $k_2 = 9.3 \times 10^9 \text{ s}^{-1}$ calculated for the aryl oxide expulsion from the T^\pm intermediate. Thus, k_3 for the decomposition process is partially rate-determining.

Kinetic studies of the NPA aminolysis by PEI performed in a 42.8 (w/w) % $\text{CH}_3\text{CN}/\text{H}_2\text{O}$ mixture at $pH^* = 6.88$ agree with the proposed mechanism. Instead of a saturation behavior like that observed in water, a linear dependence of k_{obs} on PEI concentration was found with a 1.5×10^3 -fold deceleration. The presence of the organic solvent would prevent the weak substrate–polyelectrolyte interactions, and the aminolysis reaction proceeds without a preassociation step. Since PEI is more soluble in water than in CH_3CN , in this mixed solvent a preferential absorption of water occurs on the polymer surface, which causes a higher polarity than in the bulk solvent.²⁷ The neutral substrate solvated hydrophobically by CH_3CN is not attracted to the hydrated polymer surface due to the incompatibility of the two solvent spheres. This result and the similar basicity of PEI in water and in mixed solvents at $pH = 6.88$ (see pK_n in Table 1) suggest that the deceleration effect can be explained by an unfavorable partition of

Scheme 3



Ar = C_6H_4 -2- NO_2 for **NPA**; Ar = C_6H_3 -2,4- NO_2 for **DNPA**; Ar = C_6H_3 -2- NO_2 -4- SO_3^- for **ANBS**; Ar = C_6H_2 -2,4- NO_2 -3- CO_2^- for **ADNB**

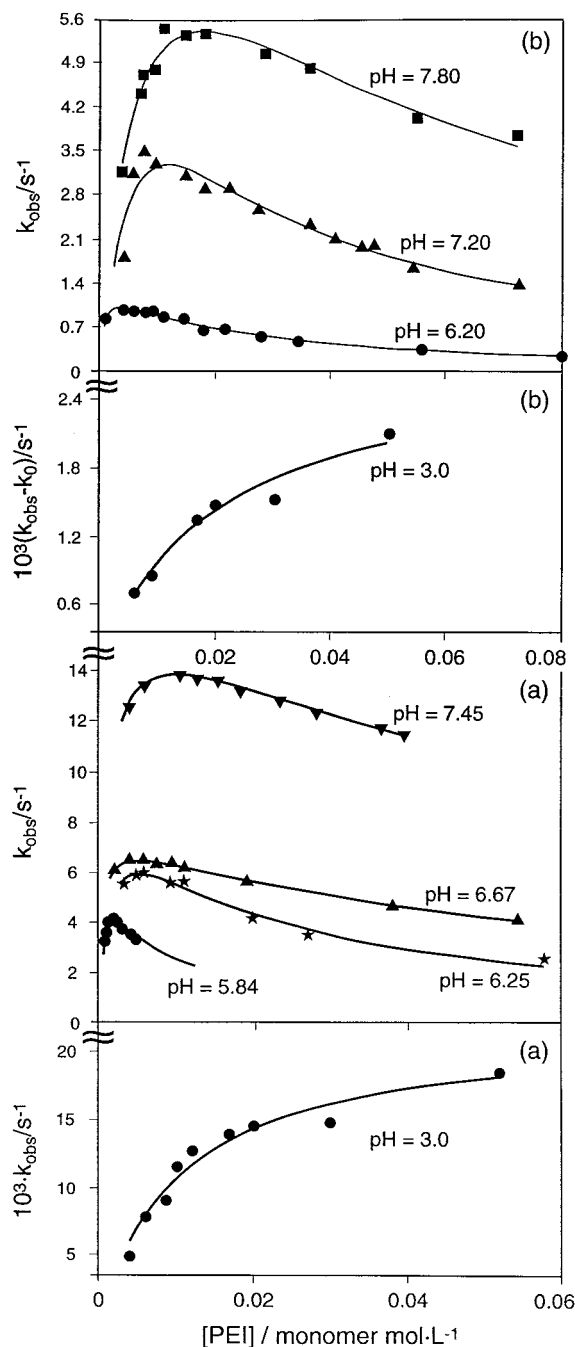
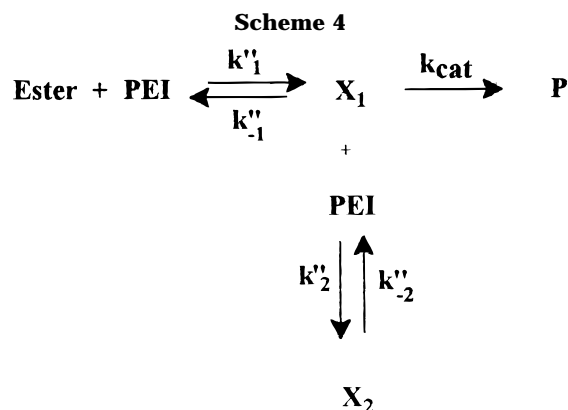


Figure 3. Dependence of the pseudo-first-order rate constant (k_{obs}) on the PEI concentration for the aminolysis of ADNB (a) and ANBS (b) at various pH at 25 °C. The points are experimental and the lines represent the best fit obtained by means of eq 3 using the parameters given in Table 1.

the charged intermediate T^\pm to the products, as observed for the aminolysis of phenyl acetates in aprotic solvents.²⁸

Aminolysis of 4-Acetoxy-3-nitrobenzenesulfonate (ANBS) and 3-Acetoxy-2,6-dinitrobenzoic Acid (ADNB). The kinetics of the aminolysis of anionic esters²⁹ show a different behavior according to the pH value of the reaction. At pH > 8.40 the pseudo-first-order rate constants (k_{obs}) reveal the usual saturation process with increasing PEI concentration. However, at lower pH values, the rate constants pass through a maximum and then decrease, indicating an apparent polyelectrolyte inhibition.³¹ Some representative examples are reported in Figure 3. These results can be

interpreted as follows. In the protonation process the distribution of charges on the primary, secondary, and tertiary amino groups of branched PEI is determined by the pK_i intrinsic ionization constant values of 9.5, 8.5, and 7.5^{10b} as well as the ratio in which they are present (1:2:1). In the region with a low degree of ionization ($\alpha < 0.29$, $pH \geq 8.40$) a large fraction of free amino groups are present. Upon increasing the macroion concentration, the rate constant increases since the electrostatic field, created by the positive charges, attracts the anionic substrates close to the polymer chain, finally reaching a state of saturation. However, at lower pH values, the number of protonated sites and doublets of vicinal charges^{10b} increases considerably. Therefore, the anionic substrate can bind itself with nonproductive sites far away from the nucleophilic groups responsible for the reaction, and consequently, the rate constant decreases. A simple mechanism that can explain this behavior involves two different substrate–polyelectrolyte complexes X_1 and X_2 (Scheme 4)³²



Only the complex X_1 (binding constant $K_1 = K'_1/K'_{-1}$) is considered capable of breaking down into the products of the reaction. The complex X_1 could in turn associate with another PEI macroion to give the unreactive complex X_2 (inhibition constant $K_2 = K'_2/K'_{-2}$). If $[PEI]_0$ and $[S]_0$ are the initial polyelectrolyte and substrate concentrations and being $[PEI]_0 \gg [S]_0$ in our experiments, it is valid to consider that $[PEI] = [PEI]_0 - [X_1] - [X_2] \approx [PEI]_0$ and $[S]_t = [S]_0 - [X_1] - [X_2]$, where $[S]_t$ is the stoichiometric substrate concentration and $[X_1]$ and $[X_2]$ are the complex concentrations. The following equations are obtained for the rate of aminolysis of the two esters:

$$v = -d[\text{ester}]/dt = k_{\text{obs}}[S]_t = k_{\text{cat}}[X_1] \quad (2)$$

$$k_{\text{obs}} = \frac{k_{\text{cat}} K_1 [\text{PEI}]}{1 + K_1 [\text{PEI}] + K_1 K_2 [\text{PEI}]^2} \quad (3)$$

The kinetic model proposed above offers a plausible interpretation of our experimental results as shown by the good agreement between the experimental points and the curves calculated by means of eq 3 (see Figure 3). The best fitting values of K_1 , K_2 , and k_{cat} are listed in Table 1. When the pH value decreases, the association (K_1) and the inhibition (K_2) constants increase, and the curve maximum is shifted to a lower polyelectrolyte concentration. This fact can be explained considering that the maximum of the curves is given by the derivative of eq 3: $[\text{PEI}]_{\text{max}} = (K_1 K_2)^{-1/2}$. The binding

constants K_1 , which are on average 2–200 times higher than K_2 , decrease from $3.8 \times 10^3 \text{ M}^{-1}$ at $\text{pH} = 4.00$ to 4.0 M^{-1} at $\text{pH} = 10.70$ for the ANBS. A similar behavior is observed also for the ADNB. However, when $\text{pH} = 3.00$ is attained, only the saturation kinetics are observed for both esters (see Figure 3). These findings are a consequence of the electrostatic nature of the phenomenon. At $\text{pH} = 3.00$ no further protonation^{10b} of the macroin is possible, and the excess HCl provides chloride counterions which shield the positive charges on the macroion, decreasing the extent of substrate binding⁶ and also suppressing the inhibition.

The effect of the substrate inhibition has been already explained by Overberger et al.,^{17b} in the hydrolysis of 3-nitro-4-dodecanoyloxybenzoic acid catalyzed by the poly(1-methyl-5-vinylimidazole), in terms of multiplicity of catalytic sites on the polyelectrolyte.

The accelerating effect of the polyamine calculated by the ratio $(k_{\text{cat}}K_1)/k_2$ is about 1×10^6 at $\text{pH} = 4.00$ for both esters and decreases to 18 for the ANBS and 23 for the ADNB at $\text{pH} = 10.33$.

The thermodynamic parameters calculated for the anionic ester ANBS (Table 2) reveal that the binding process is accompanied by a small negative enthalpy ($\Delta H = -9.6 \text{ kJ mol}^{-1}$) and a positive change in entropy ($\Delta S_u = 41 \text{ J K}^{-1} \text{ mol}^{-1}$). This large entropy value may be attributed to the release of water molecules caused by the charge neutralization between the positively charged polyelectrolyte and the anionic substrate.^{14,19} The catalytic activity of the polyamine is due to the low value of the activation enthalpy ΔH^\ddagger (20.5 kJ mol^{-1}) found for the decomposition of the complex X_1 , which however has an unfavorable entropy ΔS^\ddagger ($-159 \text{ J K}^{-1} \text{ mol}^{-1}$) in comparison with the bimolecular reaction ($\Delta S^\ddagger = -29.3 \text{ J K}^{-1} \text{ mol}^{-1}$), probably caused by the polyelectrolyte rearrangement in the intermediate complex. The proximity of the ΔF^\ddagger value found for the decomposition of the complex (68 kJ mol^{-1}) and the uncatalyzed process (72 kJ mol^{-1}) suggests that similar mechanisms are operating.

When the kinetic measurements of the aminolysis of ANBS with PEI were conducted in mixed solvent (42.8 (w/w) % $\text{CH}_3\text{CN}/\text{H}_2\text{O}$) at $\text{pH}^* = 7.20$, we observed an usual saturation behavior and the disappearance of the inhibition phenomena. Furthermore, the reaction is accelerated. The binding constant $K_1 = 1.0 \times 10^3 \text{ M}^{-1}$ results more than 6 times higher and the catalytic rate constant $k_{\text{cat}} = 21 \text{ s}^{-1}$ is more than 2 times higher than that found in aqueous solution at the same pH (see Table 1). Apart from the disappearance of the inhibition which cannot yet be explained, these results can be interpreted as follows. The anionic substrate, as well as the polyelectrolyte, in the mixed solvent is surrounded by similar hydrophilic and hydrophobic hydration spheres. Consequently, counterion binding is encouraged because of the increasing electrostatic attractive forces in a system with a polarity lower than that of water. Considering that at $\text{pH} = 7.20$, the basicity of the PEI is comparable in water, and in the mixed solvent ($\text{p}K_n = 7.05$ and $\text{p}K_n^* = 7.15$), the higher rate of the decomposition of the complex (k_{cat}) may be attributed to a greater stabilization of the transition state rather than to stabilization through the desolvation of the reagents.

Now it is appropriate to return to the question of the reaction mechanism in aqueous solution. A general mechanism that considers the experimental results of

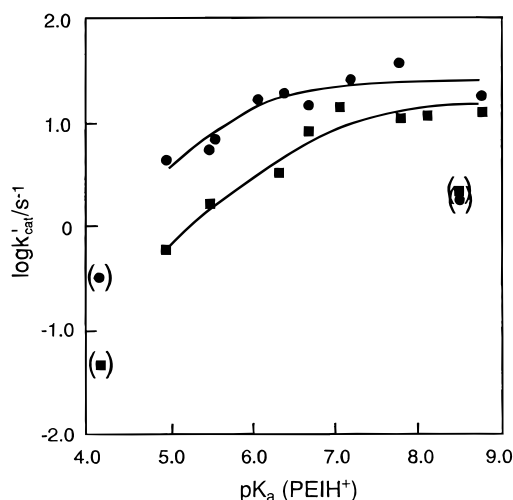


Figure 4. Brønsted-type plots of $\log k'_{\text{cat}}$ vs $\text{p}K_n$ of PEI for the aminolysis of ADNB (●) and ANBS (■) at 25°C . The points are experimental, and the lines are calculated by means of eq 4. In parentheses points not computed.³⁴

the decomposition of the complex X_1 is shown in Scheme 3. An analysis of the possible reaction pathways, such as nucleophilic (K_2), intramolecular base (K_3), and acid catalysis (K_4), takes the following arguments into account.

The Brønsted-type plots (data from Table 1) for the dependence of the decomposition rate of the complex ($\log k'_{\text{cat}}$) on $\text{p}K_n$ of PEI are not linear for both esters, as shown in Figure 4, and exhibit a transition from a relatively large sensitivity to a small sensitivity with respect to the PEI basicity. This behavior can be interpreted through the existence of a zwitterionic tetrahedral intermediate T^\pm along the reaction path. When the polyamine basicity increases, the nucleophilic attack of PEI amino groups on ester occurs with a change in the rate-determining step from the decomposition of intermediate T^\pm to its formation K_1 . By applying the steady-state approximation to the transformation of T^\pm , the equation $k'_{\text{cat}} = K_1 K_2 / (K_{-1} + K_2)$ is obtained. The curves in Figure 4 were calculated by means of a semiempirical eq 4 based on the assumptions previously mentioned.^{7,22d,e,f}

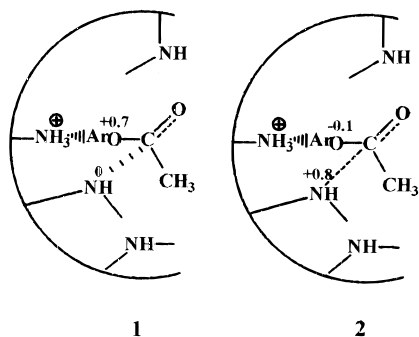
$$\log(k'_{\text{cat}}/k'_{\text{cat}}^\circ) = \beta_2(\text{p}K_n - \text{p}K_n^\circ) + \log 2 - \log[1 + 10^{(\beta_2 - \beta_1)(\text{p}K_n - \text{p}K_n^\circ)}] \quad (4)$$

$\text{p}K_n^\circ$ is the $\text{p}K_n$ at the center of the curvature ($K_{-1} = K_2$), $\log k'_{\text{cat}}^\circ$ is the corresponding value, and β_1 and β_2 are the slopes when K_1 and K_2 are the rate-determining steps. The best calculated values of these parameters are $\beta_1 = 0$, $\beta_2 = 0.75$, $\text{p}K_n^\circ = 6.90$, and $\log k'_{\text{cat}}^\circ = 0.962$ for the ANBS. Similarly, for the ADNB, values of $\beta_1 = 0$, $\beta_2 = 0.81$, $\text{p}K_n^\circ = 5.90$, and $\log k'_{\text{cat}}^\circ = 1.09$ were found.

The Brønsted-type plots for the aryl oxide ion leaving group are illustrated in Figure 5. The best fitting of the curves is obtained using the same eq 4, in which $\text{p}K_n$ and $\text{p}K_n^\circ$ are substituted by $\text{p}K_{\text{lg}}$ and $\text{p}K_{\text{lg}}^\circ$. At $\text{pH} = 8.40$ the best parameter values are $\beta_1 = 0$, $\beta_2 = -0.76$, $\text{p}K_{\text{lg}}^\circ = 5.41$, and $\log k'_{\text{cat}}^\circ = 1.61$, and at $\text{pH} = 6.67$ $\beta_{\text{lg}1} = 0$, $\beta_{\text{lg}2} = -0.83$, $\text{p}K_{\text{lg}}^\circ = 6.30$, and $\log k'_{\text{cat}}^\circ = 0.932$.

The data reported above permit us to make a tentative assignment of the "effective charges",^{22c,36} i.e., the change in the charge at a particular atom at the reaction center in the transition states, for the reaction of the

complex X_1 (see **1** and **2**).³⁷ The clear-cut changes of the charges on the ethereal oxygen of the phenoxy group, and nitrogen nucleophile, agree with the stepwise process.



The change in the rate-determining step (Figure 4) occurs at pK_n values 2.1 units lower than those found in the uncatalyzed reaction reported in ref 4 ($pK_n = 9.02$ for the ANBS and 7.94 for the ADNB). Since the lower polarity in the X_1 complex microenvironment^{1c} is not responsible for the lower pK_n found for both esters, the shift of the center of the curvature could be explained by either a better nucleofugacity of the aryl oxide ion or a lower nucleofugacity of the PEI amino group from the intermediate T^\pm in the complex. Which of the two processes occurs faster can be deduced from the calculations of the microscopic rate constants k_2 (expulsion of the ArO^- from the zwitterionic tetrahedral intermediate) and k_{-1} (expulsion of the PEI amino group moiety) (Scheme 3). Assuming the rate of ArO^- expulsion is independent of the nature and basicity of the PEI amino groups in the complex, the rate constant k_2 can be calculated by eq 5:

$$\log k_2 = 10.7 - 0.1pK_{lg} \quad (5)$$

The value -0.1 for the sensitivity of $\log k_2$ toward the leaving group basicity (pK_{lg}) is achieved by adding the charge 0.7 present on the oxygen atom of the ester in the complex⁷ to the mean value of $\beta_O = -0.8$ verified for k_2 . The constant term 10.7 is obtained from the rate constant of the ArO^- expulsion from T^\pm obtained in a model reaction: the aminolysis of the 1-acetoxy-4-methoxy pyridinium ion with methylamine.^{22e}

The rate of expulsion k_{-1} of the polymeric amine from T^\pm can be deduced by means of eq 6:

$$\log k_{-1} = 11.4 + 0.7pK_{lg} - 0.8pK_n \quad (6)$$

The parameters $\beta_O = 0.7$ and $\beta_N = -0.8$ are obtained from the charge differences of the oxygen and nitrogen atom in the transition state and in the T^\pm intermediate. The constant term of eq 6, 11.4 , was then calculated by setting $k_{-1} = k_2$ and using $pK_{lg} = 4.40$ and $pK_n = 5.90$ in the case of 3-acetoxy-2,6-dinitrobenzoic acid (ADNB).

Since the rate of phenolate ion expulsion from T^\pm is the same in the catalyzed and uncatalyzed process (see eq 6 in ref 7), it can be concluded that the nucleofugacity of the polymeric amine for T^\pm is lower in the former. This fact is supported by the ratio of k_{-1} , calculated from eq 6, to the corresponding value for the bimolecular reaction k_1 calculated by means of eq 5 in ref 7. The ratio $k_{-1}(PEI)/k_1(PEI)(KCl)$ is 1.6×10^{-2} for ANBS and 7.5×10^{-3} for the ADNB. These findings suggest that the presence of electrostatic interactions and/or hydro-

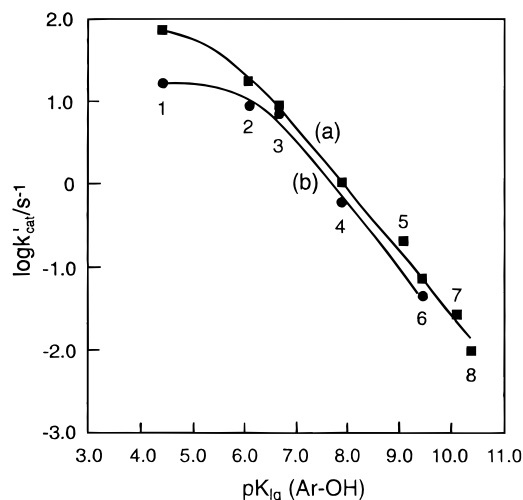


Figure 5. Brønsted-type plots of $\log k_{cat}$ vs pK_{lg} (aryl oxide ion leaving group) for the aminolysis of anionic phenyl acetates by PEI at pH 8.40 (a) and at pH 6.67 (b) at 25 °C. The points are experimental, and the lines are calculated by means of the corresponding eq 4 for the leaving group (see text). The values of k_{cat} are calculated from data reported in Table 1 and ref 6. pK_{lg} are from refs 7 and 35. The esters are in the order (1) 3-acetoxy-2,6-dinitrobenzoic acid, (2) 4-acetoxy-3-nitrobenzenesulfonate, (3) 4-acetoxy-3-nitrobenzoic acid, (4) 4-acetoxy-3-chlorobenzoic acid, (5) 5-acetoxybenzenesulfonate, (6) 4-acetoxybenzoic acid, (7) 3-acetoxybenzoic acid, and (8) 4-acetoxyphenylacetic acid.

gen bonding between the negatively charged carbonyl oxygen and positively charged ammonium groups in a tight T^\pm intermediate (Scheme 3) decreases the “push” of electrons to release the amine moiety from T^\pm . In the bimolecular aminolysis, the T^\pm intermediate is only involved in loose interactions with the polymer chain because the presence of the strong electrolyte (KCl) shields the positive charge present on the polyion.

The estimated values of k_3 in the case of ANBS (Scheme 3), indicate that the intramolecular base-catalyzed proton transfer from T^\pm , yielding an anionic intermediate T^- , is not kinetically significant (see Appendix). Only at pH = 5.0 is the calculated value for the microscopic rate constant $k_3[PEI]_i = 3.6 \times 10^{11} s^{-1}$ 30 times higher than the corresponding values obtained for the spontaneous decomposition of the T^\pm intermediate ($k_2 = 1.2 \times 10^{10} s^{-1}$) and thus could be rate-determining. The intramolecular general acid catalysis k_4 seems to be unimportant because the proton transfer from an ammonium group to T^\pm to give a cationic intermediate T^+ is never favored.

At this point the comparison of the data obtained for neutral and anionic esters permits meaningful conclusions to be drawn. First, it seems that in the catalytic process ($k_{cat}K_1$) the higher reactivity of the anionic ester ANBS compared to that of the neutral NPA at pH = 8.40 (1.2×10^3 -fold, $\Delta\Delta F^\ddagger = 17 kJ mol^{-1}$; see Table 2) arises from a more favorable free binding energy ($\Delta F_u = -21.8 kJ mol^{-1}$) as well as a much more relevant enthalpic gain ($\Delta H^\ddagger = 10.5 kJ mol^{-1}$), which exceeds the unfavorable entropy term ($\Delta S^\ddagger = -154 J K^{-1} mol^{-1}$). Second, the polyelectrolyte is capable of manifesting its catalytic power not only by accumulating substrate near the chain (K_1) but also by increasing the complex reactivity X_1 of anionic esters compared to that of the neutral ones. In fact, at pH = 4.00 (the polyelectrolyte is strongly protonated ($\alpha = 0.88$)) the $k_{cat}(ANBS)/k_{cat}^-(NPA)$ ratio is 2.9×10^3 (ref 38) while at pH = 9.10 (the

macroion is almost uncharged $\alpha = 0.14$) the ratio is reduced to 13. Similarly, the $k_{\text{cat}}(\text{ADNB})/k_{\text{cat}}(\text{DNPA})$ ratio, 4.4×10^2 at pH = 4.00 (ref 38), decreases to 1 at pH = 10.70. When the electrostatic field is strongly reduced at pH ≥ 9.10 , the rate ratio is comparable to that which is expected due to the electronic effect of the anionic substituent on the phenolic ring.³⁹

Conclusions

Despite the strong substrate–polyelectrolyte interactions which create an inhibition phenomenon, it is possible to obtain Brønsted-type plots and to describe the reaction mechanism of the aminolysis of phenyl acetates by poly(ethylenimine) as a stepwise mechanism in which a change in the rate-determining step can be recognized. The rate enhancement of anionic esters in comparison with neutral ones can be attributed to electrostatic phenomena which result in an accumulation of charged substrates around the macroion and a modification of the reactivity within the substrate–polyelectrolyte X_1 complex. The binding of the substrate releases water molecules and, the anionic ester attracted to the polymer surface, passes into a less polar environment where the tight tetrahedral intermediate T^\pm is stabilized by electrostatic and/or hydrogen bond interactions. As a consequence, the nucleofugacity of the PEI amino groups in the zwitterionic tetrahedral intermediate decreases compared to the case of the bimolecular process. In total, the reaction can be considered as the first example of a polyelectrolyte catalysis, in which the stabilization of an intermediate can be explained by a “solvation substitution”, hypothesized also for the enzyme catalysis.⁴¹

Acknowledgment. We thank Professor Andrew Williams (University of Kent) and Roberto Sartorio (University of Napoli) for helpful suggestions. We acknowledge financial support from the University of Bologna: funds for selected research topics and Fondi Ricerca Istituzionale (ex quota 60%).

Appendix

According to the hypotheses previously assumed for the bimolecular aminolysis with PEI, and following the same procedure,⁷ it is possible to evaluate the microscopic rate constants K'_2 , K'_3 , and K'_4 for the reaction pathways in Scheme 3 (ref 24) only relative to NPA and ANBS. Nevertheless, we believe that the conclusions can be extended to DNPA and ADNB due to their higher reactivity.

2-Nitrophenyl Acetate (NPA). The rate constant for the spontaneous decomposition of the T^\pm intermediate was calculated from eq 5: $K'_2 = 9.3 \times 10^9 \text{ s}^{-1}$ with a $pK_{\text{lg}} = 7.23$.

The intramolecular base catalysis was estimated by the equation $K'_3[\text{PEI}]_i$, where K'_3 is the second-order rate constant for the proton transfer from the T^\pm intermediate to an amino group of PEI to yield T^- and $[\text{PEI}]_i$ is the intramolecular free base concentration in the complex. From the relationship $pK_n(T^\pm) = pK_n(\text{PEI}) - 2.2$ (ref 7), it appears evident that the proton transfer is thermodynamically favored at every pH, and consequently the value of $K'_3 = 2 \times 10^9 \text{ M}^{-1} \text{ s}^{-1}$ is employed.^{7,25} $[\text{PEI}]_i$ can be estimated using the product $\text{EM}(1 - \alpha)$. EM is the effective molarity,^{21b,23} and $(1 - \alpha)$ represents the fraction of nonionized amino groups. It was calculated from the ratio k_{cat}/k_2 , where k_{cat} (s^{-1})

is the first-order rate constant for the decomposition of the complex (see Table 1) and k_2 ($\text{M}^{-1} \text{ s}^{-1}$) is the second-order rate constant for the bimolecular aminolysis in PEI measured in 1 M KCl. At pH = 9.10 ($pK_n = 8.30$) with $k_{\text{cat}} = 0.82 \text{ s}^{-1}$ and $k_2 = 0.043 \text{ M}^{-1} \text{ s}^{-1}$ (ref 20), an effective molarity $\text{EM} = k_{\text{cat}}/k_2 = 0.82/0.043 = 19 \text{ M}$ is obtained. Since at pH = 9.10, $(1 - \alpha) = 0.86$, the intramolecular free base concentration $[\text{PEI}]_i$ is $19 \times 0.86 = 16.3 \text{ M}$, and consequently $K'_3[\text{PEI}]_i = 16.3 \times 2 \times 10^9 = 3.3 \times 10^{10} \text{ s}^{-1}$ can be calculated. At pH = 4.55, with $pK_n = 5.19$, the value of $k_2 = 1.6 \times 10^{-5} \text{ M}^{-1} \text{ s}^{-1}$ is obtained. Since $k_{\text{cat}} = 7.82 \times 10^{-5} \text{ s}^{-1}$, $\text{EM} = 7.82 \times 10^{-5}/1.6 \times 10^{-5} = 4.88 \text{ M}$, and being $(1 - \alpha) = 0.19$, the intramolecular free base concentration $[\text{PEI}]_i = 4.88 \times 0.19 = 0.927 \text{ M}$ and consequently $K'_3[\text{PEI}]_i = 1.8 \times 10^9 \text{ s}^{-1}$ can be calculated.

The intramolecular acid catalysis can be estimated from the equation $K'_4[\text{PEIH}^+]_i$, where K'_4 is the second-order rate constant for the proton transfer from the ammonium ion to T^\pm to yield T^+ and $[\text{PEIH}^+]_i$ is the intramolecular ammonium ion concentration in the complex. The microscopic rate constant K'_4 can be evaluated from the $pK_{\text{OH}}(T^+)$ as follows. In addition to the electronic effects on the acidity of the hydroxyl group in the T^+ intermediate formed by the attack of primary or secondary amino groups, it is also necessary to consider the electrostatic effect caused by the unshielded positive charges present on the macroion surface. We assume a maximum decrease of 2.43 units on the $pK_{\text{OH}}(T^+)$ considering that the electrostatic field does not depend on the degree of ionization.²⁶ Under these conditions and on the basis of the procedure previously reported,⁷ we estimate at pH = 9.10 ($pK_n = 8.30$) a $pK_{\text{OH}}(T^+) = 4.43$ for the T^+ intermediate resulting from a primary amino group proton transfer. At pH = 4.55 ($pK_n = 5.19$) the $pK_{\text{OH}}(T^+) = 3.59$ is obtained for the T^+ intermediate formed by a secondary amino group proton transfer. In conclusion, the intramolecular proton transfer K'_4 is not favored, while the reverse reaction pathway K'_{-4} is. Subsequently, the microscopic rate constant for the proton transfer can be estimated from the relationship $K'_4 = K'_{-4} \times 10^{pK_{\text{OH}}(T^+)}$.^{7,25} Thus, at pH = 9.10, using $K'_{-4} = 10^9 \text{ M}^{-1} \text{ s}^{-1}$ (ref 7) and $pK_{\text{OH}}(T^+) = 4.43$, a value of $K'_4 = 3.7 \times 10^4 \text{ M}^{-1} \text{ s}^{-1}$ can be calculated. The intramolecular ammonium ion concentration $[\text{PEIH}^+]_i$ is given by the product $\text{EM}\alpha$ (α is the fraction of protonated amino groups). Starting from $\text{EM} = 19 \text{ M}$ and $\alpha = 0.14$, found at pH = 9.10, the intramolecular ammonium ion concentration $[\text{PEIH}^+]_i = 19 \times 0.14 = 2.66 \text{ M}$ is calculated, and a value of $K'_4[\text{PEIH}^+]_i = 9.8 \times 10^4 \text{ s}^{-1}$ can be obtained. Similarly, at pH = 4.55, the value $K'_4 = 2.6 \times 10^5 \text{ M}^{-1} \text{ s}^{-1}$ can be calculated. Using the effective molarity $\text{EM} = 4.88 \text{ M}$ and $\alpha = 0.81$, $K'_4[\text{PEIH}^+]_i = 2.6 \times 10^5 \times 4.88 \times 0.81 = 1 \times 10^6 \text{ s}^{-1}$ is obtained.

4-Acetoxybenzenesulfonate (ANBS). The value of $K'_2 = 1.2 \times 10^{10} \text{ s}^{-1}$ for the decomposition of the T^\pm intermediate to the products is calculated from eq 5 considering a $pK_{\text{lg}} = 6.08$. Since the intramolecular proton transfer from T^\pm to an amino group of PEI yielding T^- is always favored (see above), a value of $K'_3 = 2 \times 10^9 \text{ M}^{-1} \text{ s}^{-1}$ (ref 7) was used. At pH = 10 ($pK_n = 8.48$), using $k_{\text{cat}} = 1.97 \text{ s}^{-1}$ and $k_2 = 1.04 \text{ M}^{-1} \text{ s}^{-1}$, which was calculated at the same basicity in the bimolecular aminolysis,²⁰ the effective molarity $\text{EM} = 1.97/1.04 = 1.89 \text{ M}$ results. Starting from $(1 - \alpha) = 0.97$, the intramolecular free base concentration $[\text{PEI}]_i$ is $1.89 \times$

$0.97 = 1.83 \text{ M}$, and consequently, $K_3[\text{PEI}]_i = 3.7 \times 10^9 \text{ s}^{-1}$ can be calculated. At $\text{pH} = 5.00$ ($\text{p}K_n = 5.46$) using $k_{\text{cat}} = 0.426 \text{ s}^{-1}$ and $k_2 = 6.1 \times 10^{-4} \text{ M}^{-1} \text{ s}^{-1}$ calculated from data in ref 7, the effective molarity $\text{EM} 0.426/6.1 \times 10^{-4} = 698 \text{ M}$ is obtained. Since $(1 - \alpha) = 0.26$ and $[\text{PEI}]_i = 698 \times 0.26 = 181$, the value $K_3[\text{PEI}]_i = 3.6 \times 10^{11} \text{ s}^{-1}$ can be calculated.

The intramolecular acid catalysis $K_4[\text{PEIH}^+]_i$ can be evaluated in the same way. At $\text{pH} = 10.02$ ($\text{p}K_n = 8.48$), $\text{p}K_{\text{OH}}(\text{T}^+) = 4.0$ can be calculated. Therefore, the proton transfer from an ammonium ion to T^\pm yielding the T^+ intermediate is not favored. From the equation $K_4 = K_{-4} \times 10^{\text{p}K_{\text{OH}}(\text{T}^+)}$, $K_4 = 10^9 \times 10^{-4} = 10^5 \text{ M}^{-1} \text{ s}^{-1}$ can be obtained. At this pH value with $\text{EM} = 1.89 \text{ M}$ and $\alpha = 0.03$ (see above), $[\text{PEIH}^+]_i = 1.89 \times 0.03 = 0.06 \text{ M}$ and $K_4[\text{PEIH}^+]_i = 10^5 \times 0.06 = 6 \times 10^3 \text{ s}^{-1}$ is obtained. Similarly, at $\text{pH} = 5.00$ ($\text{p}K_n = 5.46$) values of $\text{p}K_{\text{OH}}(\text{T}^+) = 2.83$ and $K_4 = 10^9 \times 10^{2.83} = 1.5 \times 10^6 \text{ M}^{-1} \text{ s}^{-1}$ can be calculated. At this pH value, $[\text{PEIH}^+]_i = 698 \times 0.74 = 517 \text{ M}$ and $K_4[\text{PEIH}^+]_i = 1.5 \times 10^6 \times 517 = 7.7 \times 10^8 \text{ s}^{-1}$ result using an effective molarity of $\text{EM} = 698 \text{ M}$ and $\alpha = 0.74$ (see above).

These results suggest that, for both esters, the paths through T^- (K_3) or T^+ (K_4) are not significant in comparison to that through T^\pm (K_2).

References and Notes

- (1) (a) Kunitake, T.; Okahata, Y. *Advances in Polymer Science*; Springer-Verlag: New York, 1976; p 159. (b) Lege, C. S.; Deyrup, J. A. *Macromolecules* **1981**, *14*, 1629, 1634. (c) Everaerts, A.; Samyn, C.; Smets, G. *Makromol. Chem.* **1984**, *185*, 1881. (d) Overberger, C. G.; Gutler, A. C. *J. Polym. Sci., Polym. Symp.* **1978**, *62*, 13.
- (2) (a) Overberger, C. G.; Salamone, J. C. *Acc. Chem. Res.* **1969**, *2*, 117. (b) Klotz, I. M. In *Enzyme Mechanisms*; Page, M. I., Williams, A., Eds.; Royal Society of Chemistry: London, 1987; p 14.
- (3) Okubo, T.; Ise, N. *Adv. Polym. Sci.* **1977**, *25*, 136.
- (4) Nango, M.; Klotz, I. M. *J. Polym. Sci., Polym. Chem. Ed.* **1978**, *16*, 1265.
- (5) (a) Overberger, C. G.; Pierre, T. St.; Vorchheimer, N.; Lee, J.; Yaroslavsky, S. *J. Am. Chem. Soc.* **1965**, *87*, 296. (b) Overberger, C. G.; Smith, T. W. *Macromolecules* **1975**, *8*, 401.
- (6) Arcelli, A.; Concilio, C. *J. Chem. Res.* **1992**, (S) 8-9; (M) 201-206.
- (7) Arcelli, A.; Concilio, C. *J. Org. Chem.* **1996**, *61*, 1682.
- (8) Fernandez-Prini, R.; Baumgartner, E.; Turyn, D. *J. Chem. Soc., Faraday Trans. 1* **1978**, 1196.
- (9) Jencks, W. P.; Gilchrist, M. *J. Am. Chem. Soc.* **1966**, *88*, 104.
- (10) (a) Bloys van Treslong; Moonen, P. *J. Recl. Trav. Chim. Pays-Bas* **1978**, *97*, 22. (b) Bloys van Treslong, C. *J. Recl. Trav. Chim. Pays-Bas* **1978**, *97*, 13. (c) Bloys van Treslong, C. G.; Staverman, A. *J. Recl. Trav. Chim. Pays-Bas* **1974**, *93*, 171. (d) Kobayashi, S.; Hiroishi, K.; Tokunoh, M.; Saegusa, T. *Macromolecules* **1987**, *20*, 1496.
- (11) Bates, G. *J. Res. Natl. Bur. Stand. A* **1962**, *66*, 179.
- (12) Rondini, S.; Mussini, P. R.; Mussini, T. *Pure Appl. Chem.* **1987**, *59*, 1549.
- (13) Guggenheim, E. A. *Philos. Mag.* **1926**, *2*, 538.
- (14) Kauzman, W. *Adv. Protein Chem.* **1959**, *14*, 1.
- (15) Kunitake, T.; Shinkai, S. *J. Am. Chem. Soc.* **1971**, *93*, 4256.
- (16) (a) Johnson, R. S.; Walder, A. J.; Klotz, I. M. *J. Am. Chem. Soc.* **1978**, *100*, 5159. (b) Johnson, R. S.; Klotz, I. M. *Biopolymers* **1979**, *18*, 313.
- (17) Overberger, C. G.; Smith, T. W. *Macromolecules* **1975**, *8*, (a) 407, (b) 416.
- (18) Kunitake, T.; Sakamoto, T. *Bull. Soc. Chem. Jpn.* **1979**, *52*, 2402.
- (19) Kollman, P. In *The Chemistry of Enzyme Action*; Page, M. I., Ed.; Elsevier: New York, 1984; p 55.
- (20) The values of k_2 are calculated from equation $\log k_2 = 1.1\text{p}K_n - 10.5$ (k_2 is obtained from data reported in ref 7).
- (21) Jencks, W. P. *Catalysis in Chemistry and Enzymology*; McGraw-Hill: New York, 1969; (a) p 463, (b) p 7.
- (22) (a) Jencks, W. P.; Gilchrist, M. *J. Am. Chem. Soc.* **1968**, *90*, 2622. (b) Satterthwait, A. C.; Jencks, W. P. *J. Am. Chem. Soc.* **1974**, *96*, 7018. (c) Gresser, M. J.; Jencks, W. P. *J. Am. Chem. Soc.* **1977**, *99*, 6963. (d) Castro, E. A.; Ureta, C. *J. Org. Chem.* **1990**, *55*, 1676. (e) *J. Org. Chem.* **1989**, *54*, 2153. (f) Castro, A.; Cubillos, M.; Santos, J. G. *J. Org. Chem.* **1994**, *59*, 3572.
- (23) Kirby, A. J. *Adv. Phys. Org. Chem.* **1980**, *17*, 183.
- (24) The symbols T^\pm , T^- , and T^+ are related to the formation of charges and to the proton transfer in the adduct.
- (25) Eigen, M. *Angew. Chem., Int. Ed. Engl.* **1964**, *3*, 1.
- (26) Morishima, Y.; Kobayashi, T.; Nozakura, S.-i. *Macromolecules* **1988**, *21*, 101.
- (27) Sugimura, M.; Okubo, T.; Ise, N. *Macromolecules* **1981**, *14*, 124.
- (28) Menger, F. M.; Vitale, A. C. *J. Am. Chem. Soc.* **1973**, *95*, 4931.
- (29) The $\text{p}K_{\text{COOH}}$ of ADNB, calculated from equation $\text{p}K = 2.21 - 0.91\sum\sigma$ (ref 30), is 0.1; at the lowest pH value investigated ($\text{pH} = 3.00$) the substrate is already present as an anion.
- (30) Perrin, D. D.; Dempsey, B.; Serjeant, E. P. *pKa Predictions for Organic Acids and Bases*; Chapman and Hall: London, 1981; (a) p 126, (b) p 109.
- (31) The presence of an anionic substrate does not induce conformational changes of the polyelectrolyte, as proved by the titration curves performed with added phenol (reaction product). PEI basicity is not substantially modified by the presence of the substrates. This fact can be deduced by the small decrease in pH values (0.05–0.15) observed in the titration curves of PEI 2.5×10^{-3} monomer mol L^{-1} performed in the presence of 3-nitro-4-hydroxybenzenesulfonate and/or 3-hydroxy-2,6-dinitrobenzoic acid (sodium salts) ($5 \times 10^{-5} \text{ M}$), respectively.
- (32) It should be emphasized that Scheme 4, as well as Scheme 2, represents a simplification of a range of interactions between the esters and the polyelectrolyte which involves the formation of various reactive and unreactive complexes with different binding constants and rates of decomposition.
- (33) From data reported in Table 1 in ref 7, the values of $k_2 = 2.8 \times 10^{-4}$ and $1.54 \times 10^{-3} \text{ M}^{-1} \text{ s}^{-1}$ at $\text{pH} = 4.00$ and $k_2 = 7.2$ and $28.6 \text{ M}^{-1} \text{ s}^{-1}$ at $\text{pH} = 10.00$ are calculated for ANBS and ADNB, respectively.
- (34) The data points at $\text{p}K_n = 4.18$ ($\text{pH} = 3.00$) and at $\text{p}K_n = 8.48$ ($\text{pH} = 10.02$) (not computed) deviate negatively from the curves—the former owing to the HCl in excess (see text) and the latter as a consequence of a nonmonotonic increase of substrate macroion binding (K_1), as found for DNPA.
- (35) Arcelli, A.; Concilio, C. *J. Chem. Soc., Perkin Trans. 2* **1989**, 887.
- (36) Williams, A. *Adv. Phys. Org. Chem.* **1992**, *27*, 1.
- (37) We assume that the charges on the reagents and on the complex X_1 (Scheme 3) are the same as those on the components in the bimolecular reaction (see Appendix in ref 7). The effective charges on the oxygen and nitrogen atoms are estimated from the values of the slopes of the Brønsted plots for the nucleophilic attack (β_N) and for the aryl oxide ion leaving group (β_O) above calculated. So the effective charge on the oxygen and nitrogen atoms in the transition state **1** are obtained by adding the values of $\beta_O = 0$ and $\beta_N = 0$ (relative to the Brønsted plots when $K_{\text{cat}} = K_1$) to the charges on the atoms (0.7 for oxygen and 0 for nitrogen). Likewise, the charges -0.1 on the oxygen and 0.8 on nitrogen in the transition state **2** (when $K_{\text{cat}} = K_1(K_2/K_{-1})$) were obtained by adding the mean value of $\beta_O = -0.8$ to the charge 0.7 on the oxygen and the value $\beta_N = 0.8$ to the charge 0 on the nitrogen of the complex X_1 .
- (38) The values for NPA at $\text{pH} = 4.00$, $k_{\text{cat}} = 2.42 \times 10^{-5} \text{ s}^{-1}$, and for DNPA, $k_{\text{cat}} = 1.2 \times 10^3 \text{ s}^{-1}$, were extrapolated from data reported in Table 1.
- (39) By means of the Hammett equation $\log k/k_0 = \rho\sigma$, considering $\rho = 2$ as in aminolysis reactions with simple amines,⁴⁰ a 6-fold rate increase can be calculated for the complex decomposition of ANBS ($\sigma(4\text{-SO}_3^-) = 0.39^{30b}$) in comparison with NPA and a 1.5-fold increase of ADNB ($\sigma(3\text{-COO}^-) = 0.09^{30b}$) over DNPA.
- (40) St. Pierre, T.; Jencks, W. P. *J. Am. Chem. Soc.* **1968**, *90*, 3817.
- (41) Warshel, A.; Aquis, J.; Creighton, S. *Proc. Natl. Acad. Sci.* **1989**, *86*, 5820.